MATERIALE PLASTICE
https://revmaterialeplastice.ro
https://doi.org/10.37358/Mat.Plast.1964

CC BY

Flexural Strength Analysis and Optimisation of PP Model Based on ME-3DP Technology

CHEN WANG[1,2]*, XIAOWEN WANG[1,2], JIAHAO YU[2], HANYI HUANG[1,2]
[1] College of Furnishings and Industrial Design, Nanjing Forestry University, Nanjing, 210037, China
[2] Jiangsu Co-Innovation Center of Efficient Processing and Utilization of Forest Resources, Nanjing Forestry University, Nanjing, 210037, China

Abstract: *Polypropylene (PP) is a commonly used raw material for the production of 3D printing composite filament, which has many advantages, such as low density, insulation, chemical resistance, and environmental friendliness, but its mechanical strength is poor, which affects the comprehensive performance of the 3D printing PP model. In order to effectively improve the flexural strength of material-extrusion-based 3D printing (ME-3DP) PP model, this study investigated the influence of three printing parameters (infill rate, extrusion speed, platform temperature) on the flexural strength of the 3D printed PP model through the three-point support flexural test. The results show that the flexural strength of 3D printed PP model gradually increases with the increase of the infill rate, the decrease of the extrusion speed, and the increase of the platform temperature; the degree of influence of the three parameters on the flexural strength of the 3D printed PP model is as follows: infill rate > extrusion speed > platform temperature; the optimal combination of the printing parameters is as follows: infill rate (90%), extrusion speed (20 mm/s), and platform temperature (70°C). The flexural strength of the 3D printed PP model fabricated according to the optimal printing parameters is 41.7 MPa, which is the maximum value in the orthogonal experiment, verifying the reliability of the experiment results.*

Keywords: *Printing parameters, ME-3DP, PP model, flexural strength*

1. Introduction

Polypropylene (PP) is a thermoplastic made from the polymerisation of propylene monomers, which has the advantages of low density, insulation, chemical resistance and environmental friendliness, making it a unique advantage among many plastics, and has a wide range of applications in the consumer goods field [1–3]. PP as a substrate, adding toughening agent (such as acrylonitrile butadiene styrene or chlorinated polyethylene), inorganic fillers (talcum powder or calcium carbonate), coupling agent (sodium stibnate or silane) and other raw materials, through the melt blending and then drawing to make PP composite filament, will be used in MEX 3D printing, is a new direction of application of PP plastic [4–6].

Material-extrusion-based 3D printing (ME-3DP) is a technology that prints thermoplastic plastics into solid models by layer-by-layer stacking, which is one of the lowest-cost and most widely used additive manufacturing technologies [7,8]. Models with good chemical resistance and environmental friendliness can be manufactured using PP filament and ME-3DP technology. However, 3D printed PP model usually has poor mechanical strength, which is related to the brittleness of the PP filament itself on the one hand, and on the other hand, the printing parameters also have a significant influence on the mechanical strength of the PP model [9,10].

In order to effectively improve the mechanical strength of 3D printed PP models, this study selected the representative flexural strength of mechanical strength as the experimental index, and carried out experimental analysis from the direction of optimising printing parameters [11]. Three printing parameters (infill rate, extrusion speed, and platform temperature) that have an obvious influence on

*email: wc559@njfu.edu.cn

the flexural strength of the PP model were selected, and the specific role of each printing parameter and the optimal combination of printing parameters were analysed through single-factor and orthogonal experiments, which provide references for the better application of PP filament in ME-3DP technology.

2. Materials and methods

2.1. Materials

The PP filament (1.75 mm diameter, green, Anycubic, Shenzhen, China) was used for rapid prototyping by ME-3DP technology.

2.2. Specimen preparation

Referring to the standard ISO 178-2019, the rectangular specimen (shown in Figure 1) was designed in SolidWorks software with the following dimensions: length (l) of 160 mm, width (w) of 15 mm, and height (h) of 8 mm [12]. The desktop-level material-extrusion-based 3D printer (0.4 mm nozzle diameter, Anycubic, Shenzhen, China) was used to complete the rapid prototyping of the rectangular specimen. The general printing parameters of the 3D printer were set as follows: extrusion temperature (220°C), infill structure (grid), extrusion rate (100%), and layer height (0.2 mm) [13].

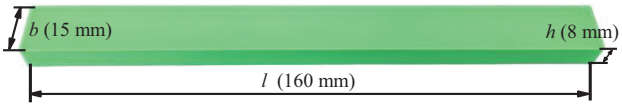

Figure 1. The rectangular specimen

The specimens prepared in this study were divided into two types: one was single-factor experiment specimens, each single-factor experiment had three groups of specimens (three parallel specimens in each group). The other one was orthogonal experiment specimens, which selected infill rate, extrusion speed, and platform temperature among the printing parameters as the influencing factors, and designed a three-factor, three-level (L_9) orthogonal experiment. The factor-level table is shown in Table 1, in which factor A represents the infill rate, factor B represents the extrusion speed, and factor C represents the platform temperature. A total of nine groups of experiments (three parallel specimens in each group) were conducted in the orthogonal experiment. The above two types of specimens had the same conditions of material, size, printing equipment, and general printing parameters.

Table 1. Factor-level table

Levels	*A* (%)	*B* (mm/s)	*C* (°C)
1	30	20	50
2	60	40	60
3	90	60	70

2.3. Performance test

The flexural strength test in this study was conducted using a three-point support flexural test, which was carried out at 20°C room temperature in the following steps: firstly, the rectangular specimen was placed on the two supports of the three-point flexural fixture (with a span L of 130 mm) to ensure that the specimen was centred [14]. Then, the universal mechanical testing machine (AG-X, 20 kN, Shimadzu, Kyoto, Japan) was started and the flexural load was applied at a loading rate of 2 mm/min. The test was stopped when the specimen broke, and the value of the maximum load F_{max} was recorded. Finally, the

flexural strength σ was calculated based on F_{max} using the following formula: $\sigma = \frac{3F_{max}L}{2wh^2}$, where F_{max} is the maximum load, L is the span, w is the width of the rectangular specimen, and h is the height of the rectangular specimen [15].

3. Results and discussions

3.1. Influence of infill rate on flexural strength of 3D printed PP model

Setting the extrusion speed of 20 mm/s and platform temperature of 70°C, the flexural strength of 3D printed PP models with different infill rates (30%, 60%, and 90%) was tested, and the test results are shown in Figure 2. As seen in Figure 2, the flexural strength of the 3D printed PP model increases with the increase of the infill rate. The flexural damage region of 3D printed PP model is located below the neutral surface of the model, because when the PP model is subjected to flexural load, the bottom surface of the model generates the largest flexural positive stress under the action of tensile force, and the flexural positive stress destroys the force between the molecular chains of the PP filaments, resulting in the fracture of filament body, and eventually lead to brittle fracture of the PP model [16–18]. When the infill rate increases, the number of filament bodies increases in the direction of the flexural positive stress, and the bonding area between adjacent layers of filaments increases, leading to an increase in the destructive stress (load) required to break the molecular chains of PP filaments, and therefore an increase in the flexural strength of 3D printed PP model [19].

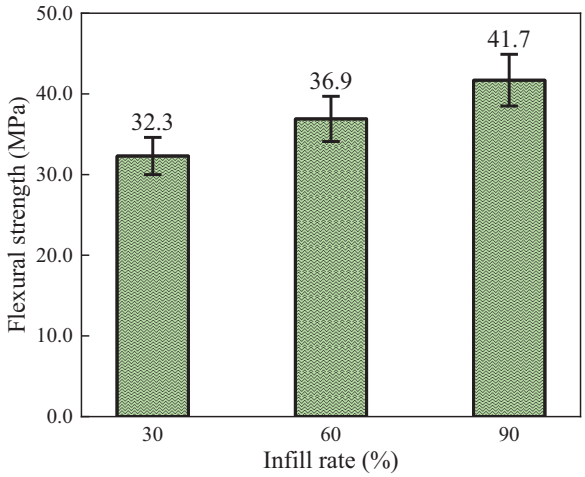

Figure 2. Influence of infill rate on flexural strength of 3D printed PP model

3.2. Influence of extrusion speed on flexural strength of 3D printed PP model

Setting the infill rate of 90% and platform temperature of 70°C, the flexural strength of 3D printed PP models at different extrusion speeds (20, 40, and 60 mm/s) was tested, and the test results are shown in Figure 3. As seen in Figure 3, the flexural strength of the 3D printed PP model increases as the extrusion speed decreases. This is because, as the extrusion speed decreases, the flow time of the molten PP filament on the surface of the adjacent layer filament increases, the spreading area increases, and the interlayer adhesion performance improves [20]. In addition, the slower the extrusion speed, the longer the contact time between the high-temperature nozzle (220°C) and the extruded filament, and the more heat is conducted from the nozzle to the filament, which further promotes the diffusion and cross-linking between the adjacent layer filament molecules, thus improving the interlayer adhesion performance of 3D printed PP model and increasing its flexural strength [21].

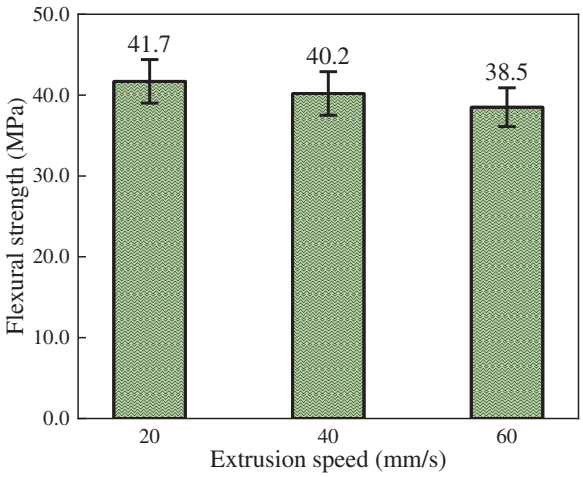

Figure 3. Influence of extrusion speed on flexural strength of 3D printed PP model

3.3. Influence of platform temperature on flexural strength of 3D printed PP model

Setting the infill rate of 90% and extrusion speed of 20 mm/s, the flexural strength of 3D printed PP models at different platform temperatures (50, 60, and 70°C) was tested, and the test results are shown in Figure 4. As seen in Figure 4, the flexural strength of the 3D printed PP model increases with the increase in platform temperature. Due to the relatively high thermal shrinkage (1.5%~2.0%) of PP filament, the problem of interlayer cracking is prone to occur during 3D printing [22]. By increasing the platform temperature, a temperature field with higher heat flow density can be formed in the closed 3D printer chassis, which increases the temperature of the PP model during the printing process, enhances the interlayer bonding performance, and avoids the interlayer cracking problem, so the flexural strength of the 3D printed PP model increases [23].

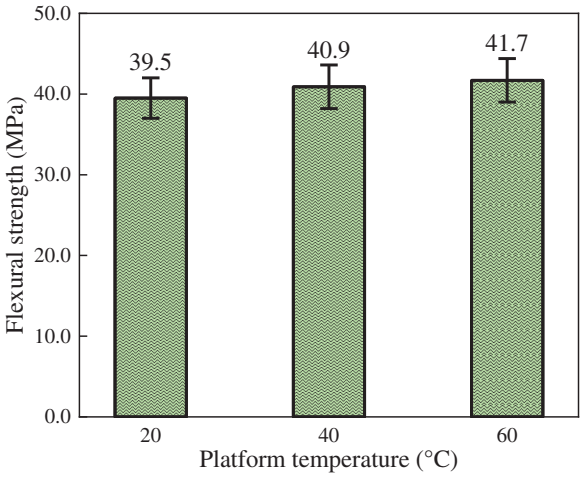

Figure 4. Influence of platform temperature on flexural strength of 3D printed PP model

3.4. Analysis of orthogonal experiment

Nine groups of orthogonal experiment specimens were tested for flexural strength, and to ensure the accuracy of the data, the flexural strength (F_n) of each group was calculated from the average of the flexural strengths of three parallel specimens, and the results of the orthogonal experiments are shown in Table 2. As seen in Table 2, the flexural strengths of 3D printed PP models showed

significant differences under different printing parameters. The maximum flexural strength of 41.7 MPa was obtained for specimen No. 7, and the minimum flexural strength of 30.8 MPa was obtained for specimen No. 3.

Table 2. Orthogonal experiment table

Number (n)	A (%)	B (mm/s)	C (°C)	F_n (MPa)
1	30	20	50	31.5
2	30	40	60	31.2
3	30	60	70	30.8
4	60	20	60	35.9
5	60	40	70	35.6
6	60	60	50	33.2
7	90	20	70	41.7
8	90	40	50	38.2
9	90	60	60	37.5

The optimal combination of printing parameters for the 3D printed PP model was determined by range analysis (see Table 3). The mean value (k_n) is used to measure the degree of influence of the three factors on the flexural strength of 3D printed PP models at different levels [24]. The range value (R) reflects the degree of influence of changes in the level of the factors on the test results, and the larger the value of the range, the more significant the influence of the changes in the factors on the experiment results [25].

Table 3. Range analysis table

Range parameters	A	B	C
k_1	93.5	109.1	102.9
k_2	104.7	104.9	104.6
k_3	117.4	101.5	108.1
R	23.9	7.6	5.2

From Table 3 and Figure 5, it can be seen that according to the sorting of R values, the influence of printing parameters on the flexural strength of 3D printed PP model is as follows: infill rate > extrusion speed > platform temperature; A_3 (90%) is the optimal parameter in factor A, as the k_3 value of factor A is the highest in the range analysis table; B_1 (20 mm/s) is the optimal parameter in factor B, as the k_1 value of factor B is the highest in the range analysis table; C_3 (70°C) is the optimal parameter in factor C, as the k_3 value of factor C is the highest in the range analysis table. The optimal combination of printing parameters is $A_3B_1C_3$, which includes infill rate (90%), extrusion speed (20 mm/s), and platform temperature (70°C), and the flexural strength of 3D printed PP model made according to these printing parameters is 41.7 MPa, which is the maximum value in the orthogonal experiment, indicating that $A_3B_1C_3$ is the optimal solution.

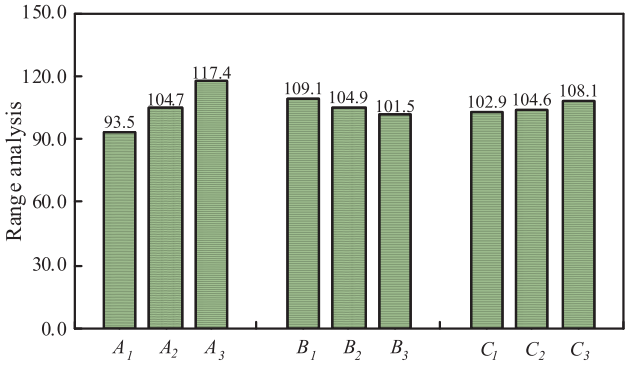

Figure 5. Range analysis diagram

4. Conclusions

In order to effectively improve the flexural strength of material-extrusion based 3D printing PP model, three printing parameters (infill rate, extrusion speed, and platform temperature), which had obvious influence on the flexural strength of 3D printed PP model were selected, and the specific role of each printing parameter and the optimal combination of printing parameters were analysed by single-factor and orthogonal experiments. The results show that the flexural strength of 3D printed PP model gradually increases with the increase of the infill rate, the decrease of the extrusion speed, and the increase of the platform temperature; the degree of influence of the three parameters on the flexural strength of the 3D printed PP model is as follows: infill rate > extrusion speed > platform temperature; the optimal combination of the printing parameters is as follows: infill rate (90%), extrusion speed (20 mm/s), and platform temperature (70°C).

Acknowledgement: Not applicable.

Funding Statement: The authors received no specific funding for this study.

Author Contributions: The authors confirm contribution to the paper as follows: study conception and design: Chen Wang; data collection: Xiaowen Wang; analysis and interpretation of results: Jiahao Yu; draft manuscript preparation: Hanyi Huang. All authors reviewed the results and approved the final version of the manuscript.

Availability of Data and Materials: The data that support the findings of this study are available from the Corresponding Author, [Chen Wang], upon reasonable request.

Ethics Approval: Not applicable.

Conflicts of Interest: The authors declare no conflicts of interest to report regarding the present study.

References

1. Yang ZZ, Feng XH, Xu M, Rodrigue D. Printability and properties of 3D printed poplar fiber/polylactic acid biocomposites. BioResources. 2022;16(2):2774–88. doi:10.15376/biores.16.2.2774-2788.
2. Yang L, Liu D, Guo R, Ji ZY, Wang XL, Shi XY. Flexibility of Diels-Alder reversible covalent bonds in fused deposition modeling 3D printing: bonding and de-bonding. Polymer. 2023;266(20):125637. doi:10.1016/j.polymer.2022.125637.
3. Wang YQ, Liu ZG, Gu HW, Cui CZ, Hao JB. Improved mechanical properties of 3D-printed SiC/PLA composite parts by microwave heating. J Mater Res. 2019;34(20):3412–9. doi:10.1557/jmr.2019.296.

4. Yilmaz M, Yilmaz NF, Kalkan MF. Rheology, crystallinity, and mechanical investigation of interlayer adhesion strength by thermal annealing of polyetherimide (PEI/ULTEM 1010) parts produced by 3D printing. J Mater Eng Perform. 2022;31(12):9900–9. doi:10.1007/s11665-022-07049-z.
5. Luo M, Tian XY, Shang JF, Zhu WJ, Li DC, Qin YJ. Impregnation and interlayer bonding behaviours of 3D-printed continuous carbon-fiber-reinforced poly-ether-ether-ketone composites. Composites Part A-Appl Sci Manufact. 2019;121(3):130–8. doi:10.1016/j.compositesa.2019.03.020.
6. Feng XH, Wu ZH, Xie YJ, Wang SQ. Reinforcing 3D print methacrylate resin/cellulose nanocrystal composites: effect of cellulose nanocrystal modification. BioResources. 2019;14(2):3701–16. doi:10.15376/biores.14.2.3701-3716.
7. Wu Y, Zhu JG, Qi Q, Cui LN. Research progress of solid wood bending softening technology. Rev Wood Res. 2022;67(6):1056–73. doi:10.37763/wr.1336-4561/67.6.10561073.
8. Zhang R, Yu LG, Chen K, Xue P, Jia MY, Hua ZT. Amelioration of interfacial properties for CGF/PA6 composites fabricated by ultrasound-assisted FDM 3D printing. Compos Commun. 2023;39(20):101551. doi:10.1016/j.coco.2023.101551.
9. Fang L, Lu XZ, Zeng J, Chen YY, Tang QH. Investigation of the flame-retardant and mechanical properties of bamboo fiber-reinforced polypropylene composites with melamine pyrophosphate and aluminum hypophosphite addition. Materials. 2020;13(2):479. doi:10.3390/ma13020479.
10. Chen YS, Zhu J. Study on bending chracteristics of fast growing eucalyptus bookcase shelves by using burgers model. Wood Res. 2019;64(1):137–44.
11. Chikkangoudar RN, Sachidananda TG, Pattar N. Influence of 3D printing parameters on the dimensional stability of polypropylene/clay printed parts using laser scanning technique. Mater Today Proc. 2022;44(6):4118–23. doi:10.1016/j.matpr.2020.10.456.
12. Hu WG, Zhao Y, Xu W, Liu YQ. The influences of selected factors on bending moment capacity of case furniture joints. Appl Sci. 2024;14(21):10044. doi:10.3390/app142110044.
13. Winter K, Wilfert J, Haeupler B, Erlmann J, Altstaedt V. Large scale 3D printing: influence of fillers on warp deformation and on mechanical properties of printed polypropylene components. Macromol Mater Eng. 2021;307(1):2100528. doi:10.1002/mame.202100528.
14. Mo XF, Zhang XH, Fang L, Zhang Y. Research progress of wood-based panels made of thermoplastics as wood adhesives. Polymers. 2022;14(1):98. doi:10.3390/polym14010098.
15. Hwang S, Fowler G, Han YS, Gardner DJ. Material property characterization of 3D printed polypropylene wood plastic composites. Polym Compos. 2024;45(17):16058–74. doi:10.1002/pc.28890.
16. Liu X, Wu ZH, Zhang JL, Ge SS. Tensile and bending properties and correlation of windmill palm fiber. BioResources. 2017;12(2):4342–51. doi:10.15376/biores.12.2.4342-4351.
17. Wang XH, Wu Y, Chen H, Zhou XY, Zhang ZK, Xu W. Effect of surface carbonization on mechanical properties of LVL. BioResources. 2019;14(1):453–63. doi:10.15376/biores.14.1.453-463.
18. Li S, Hu WG. Study on mechanical strength of cantilever handrail joints for chair. BioResources. 2023;18(1):209–19. doi:10.15376/biores.18.1.209-219.
19. Fang L, Xiong XQ, Wang XH, Chen H, Mo XF. Effects of surface modification methods on mechanical and interfacial properties of high-density polyethylene-bonded wood veneer composites. J Wood Sci. 2017;63(1):65–73. doi:10.1007/s10086-016-1589-9.
20. Qi YQ, Sun Y, Zhou ZW, Huang Y, Li JX, Liu GY. Response surface optimization based on freeze-thaw cycle pretreatment of poplar wood dyeing effect. Wood Res. 2023;68(2):293–305. doi:10.37763/wr.1336-4561/68.2.293305.

21. Feng XH, Yang ZZ, Wang SQ, Wu ZH. The reinforcing effect of lignin-containing cellulose nanofibrils in the methacrylate composites produced by stereolithography. Polym Eng Sci. 2022;2022(9):2968–76. doi:10.1002/pen.26077.
22. Liu Q, Gu Y, Xu W, Lu T, Li W, Fan H. Compressive properties of green velvet material used in mattress bedding. Appl Sci. 2021;11(23):11159. doi:10.3390/app112311159.
23. Zhu ZL, Buck D, Guo XL, Xiong XQ, Xu W, Cao PX. Energy efficiency optimization for machining of wood plastic composite. Machines. 2022;10(2):104. doi:10.3390/machines10020104.
24. Hu WG, Yu RZ. Mechanical and acoustic characteristics of four wood species subjected to bending load. Maderas-Ciencia y Tecnología. 2023;25:39. doi:10.4067/s0718-221x2023000100439.
25. Battegazzore D, Cravero F, Bernagozzi G, Frache A. Designing a 3D printable polypropylene-based material from after use recycled disposable masks. Mater Today Commun. 2022;32(2):103997. doi:10.1016/j.mtcomm.2022.103997.

Received: 10 June 2025; Accepted: 09 September 2025; Published: 30 September 2025